The pseudo-free 128 vertex model

1981 J. Phys. A: Math. Gen. 14 191

(http://iopscience.iop.org/0305-4470/14/1/019)

J. Phys. A: Math. Gen. 14 (1981) 191–209. Printed in Great Britain

The pseudo-free 128 vertex model†

Stuart Samuel

Lawrence Berkeley Laboratory, University of California, Berkeley, California 94720, USA

Received 21 March 1979, in final form 6 June 1980

Abstract. A new two-dimensional statistical mechanics model is solved. It is a general model with 32 free parameters. The solution uses integrals over anticommuting variables.

1. Introduction

Two fundamental papers (amuel 1978a, b) (to be referred to as I and II) have recently developed a new approach in attacking Ising-like spin models and ferroelectric systems. This paper will use the new methods to solve a new model called the pseudo-free 128 vertex model.

An enormous number of statistical mechanics problems have geometrical representations. This means that the partition function is a sum over geometrical configurations appropriately weighted by Boltzmann factors. Papers I and II show that it is sometimes possible to find a lattice fermionic-like field theory which reproduces the graphical configurations with the correct weights. The field theory is written in path integral form. The path integral for fermionic systems is an anticommuting variable one. Anticommuting variables provide a powerful new approach to statistical mechanics problems. References I and II were devoted to developing their application to interesting systems. These two papers were pedagogical. They reviewed the theory of anticommuting variables and developed ways of expressing partition functions in terms of them. Graphical methods were introduced in II that quickly calculate partition functions and anticommuting variable correlation functions. A whole class of solvable models were resolved using the new methods as a check that they did indeed work.

This paper is concerned with the pseudo-free 128 vertex model which has 32 free parameters and encompasses a wide range of systems. A close relative is the $128+8$ pseudo-free model which is even more general with 40 parameters. This is also solved in the paper.

Papers I and II systematically discussed the anticommuting variable techniques. For this reason few details of the 128 vertex model calculations are given. The model and the results are simply presented. The method of overcoming various difficulties such as the sign problems, how to get vertex weight factors, etc is straightforward. It is suggested that the reader consult references I and II.

Section 2 gives a brief description of the pseudo-free 128 vertex model, § 3 calculates its partition function, and § 4 treats the $128+8$ pseudo-free vertex model.

† Work has been supported by the High Energy Physics Division of the United States Department of Energy under contract No. W-7405-ENG-48.

Finally the Appendix discusses the minus sign problem due to anticommuting variable reorderings.

It should be mentioned that, in principle, these models can be solved using the Pfaffian methods but anticommuting variables are simpler. As noted in reference I, the integral over a quadratic action is always a Pfaffian. The anticommuting variables have the advantage of easily determining minus sign factors, of systematically organising the algebra, and of establishing a direct connection with field theory. References to Pfaffian methods can be found in I and II.

The methods of this paper should not be confused with the operator methods of Schultz *et al* (1964). Their basic objects are fermionic creation and destruction operators b_i, $b_i^{\dagger}$, which satisfy canonical commutation relations, $b_i b_j^{\dagger} + b_j^{\dagger} b_i = \delta_{ij}$. The anticommutation variables completely anticommute: $\eta_i \eta_j^{\dagger} + \eta_j^{\dagger} \eta_i = 0$. They use a transfer matrix; this paper uses a Euclidean functional integral approach.

2. The model

Ising models in zero magnetic field are, in general, related to closed polygon partition functions (CPPF's) where sides may overlap but cannot intersect. In such a CPPF, one sums over closed polygons weighting the sides by 'Bloch wall' Boltzmann factors. The two-dimensional Ising model thus has such a representation†. The Ising model is not the most general model which is easily solvable. The corners (vertices) of polygons may also be weighted, resultinvin the so-called free-fermion model described by the action of equation (I. 4.4) whose weights are given in figure (I) 11. Let $W_{(p)}$ be the weight of figure (I) 11*p*. Then the following constraint, known as the free-fermion constraint, is satisfied: $W_{(a)}W_{(h)} + W_{(b)}W_{(c)} = W_{(d)}W_{(f)} + W_{(e)}W_{(g)}$. Thus, although the free-fermion model is not the most general eight-vertex model, it is the most general easily solvable model.

It would be slightly more complicated than the basic Ising model to include one set of diagonal next-nearest neighbour interactions. Such a system is equivalent to the Ising model on a triangular lattice. It is again related to a CPPF. By weighting corners as well as sides, a free-fermion generalisation, known as the pseudo-free 32 vertex model (Sacco and Wu 1975), is obtained. They have solved this model and discussed some of its interesting submodels and critical phenomena.

When both next-nearest neighbour interactions are included, the Ising model cannot be solved. The spins sit on the sites of a square lattice (figure 1(a)) and bonds are drawn between sites which interact (figure 1(b)). The four directions inclined, horizontal, diagonal, and vertical, are respectively denoted by i, h, d, and v as shown in figure 2. The polygons of the corresponding CPPF are drawn on the lattice of figure 1(a) using the bonds of figure 1(b). The number of polygons is arbitrary. Although edges may intersect (figure 3(a)), they are not allowed to overlap (figure 3(b)). Weighting the corners of polygons results in a more general CPPF. The most general, easily solvable CPPF of this form is the pseudo-free 128 vertex model. It is the free-fermion generalisation of the next-nearest neighbour Ising model and it has 32 parameters which may be varied independently. It is thus a very general model. For example, it includes the pseudo-free 32 vertex model which, as Sacco and Wu (1975) noted, contains interesting models as subcases. Many new models are contained in the pseudo-free 128 vertex model.

† See the references in I and II.

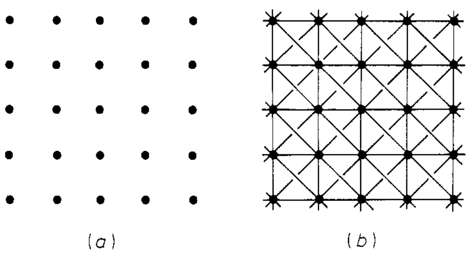

Figure 1. The square lattice.

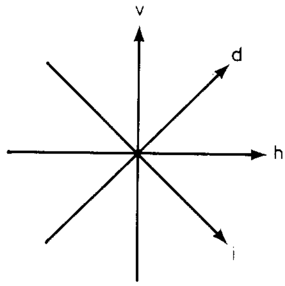

Figure 2. The four directions.

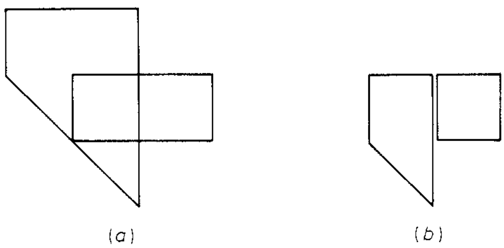

Figure 3. Allowed and forbidden configurations. The sides of polygons may intersect as in figure (a) but cannot overlap as in figure (b).

As its name implies, 128 configurations can happen at a site. This is to be compared with the eight vertex model where there are only eight. Of course, the solvable pseudo-free 128 vertex model does not assign arbitrary weights to all 128 configurations; only about one quarter of these are independent. The rest are determined by 'free-fermion constraints'. Vertex models are related to ferroelectric systems. From this point of view the pseudo-free 128 vertex model can be considered as a very general ferroelectric model.

As discussed in I and II, the partition function can be written as an anticommuting variable integral over an action, A^{128}. The action consists of three pieces, A^{128}_{wall}, A^{128}_{corner}, and A^{128}_{monomer}. They are given by

$$A^{128}_{\text{wall}} = \sum_{\alpha\beta} \left(z_{\text{i}}\eta^{\text{i}\dagger}_{\alpha\beta}\eta^{\text{i}}_{\alpha+1\,\beta-1} + z_{\text{h}}\eta^{\text{h}\dagger}_{\alpha\beta}\eta^{\text{h}}_{\alpha+1\,\beta} + z_{\text{d}}\eta^{\text{d}\dagger}_{\alpha\beta}\eta^{\text{d}}_{\alpha+1\,\beta+1} + z_{\text{v}}\eta^{\text{v}\dagger}_{\alpha\beta}\eta^{\text{v}}_{\alpha\,\beta+1}\right), \tag{2.1}$$

$$A^{128}_{\text{corner}} = \sum_{\alpha\beta}\sum_{(f,g)\in S} \left(c^1_{fg}\eta^{f\dagger}_{\alpha\beta}\eta^{g}_{\alpha\beta} + c^2_{gf}\eta^{g\dagger}_{\alpha\beta}\eta^{f\dagger}_{\alpha\beta} + c^3_{gf}\eta^{g\dagger}_{\alpha\beta}\eta^{f}_{\alpha\beta} + c^4_{gf}\eta^{g}_{\alpha\beta}\eta^{f}_{\alpha\beta}\right), \tag{2.2}$$

$$A^{128}_{\text{monomer}} = \sum_{\alpha\beta} \left(b_{\text{i}}\eta^{\text{i}}_{\alpha\beta}\eta^{\text{i}\dagger}_{\alpha\beta} + b_{\text{h}}\eta^{\text{h}}_{\alpha\beta}\eta^{\text{h}\dagger}_{\alpha\beta} + b_{\text{d}}\eta^{\text{d}}_{\alpha\beta}\eta^{\text{d}\dagger}_{\alpha\beta} + b_{\text{v}}\eta^{\text{v}}_{\alpha\beta}\eta^{\text{v}\dagger}_{\alpha\beta}\right). \tag{2.3}$$

The η's are anticommuting variables. There are four types at each site: inclined, horizontal, diagonal, and vertical ones. In addition, there is a daggered and undaggered version of each. The α and β label sites, that is, (α, β) are the cartesian coordinates of a site.

The terms in (2.1) have the graphical representation of figure 4. The conventions established in I and II are used: daggered variables and undaggered variables correspond to x's and o's, the direction of a line entering a variable determines whether it is

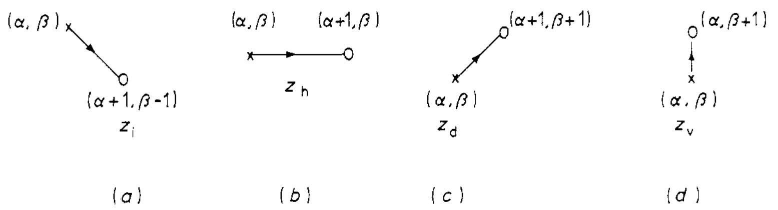

Figure 4. The wall operators.

an inclined, horizontal, diagonal, or vertical type, and arrows denote the order of bilinears. The constants, z_i, z_h, z_d, and z_v, are the Bloch wall Boltzmann factors. Each inclined, horizontal, diagonal, or vertical unit of wall is weighted by z_i, z_h, z_d, or z_v.

In equation (2.2), S is the following set of ordered pairs:

$$S=\{(\mathrm{i},\mathrm{h}),(\mathrm{i},\mathrm{d}),(\mathrm{i},\mathrm{v}),(\mathrm{h},\mathrm{d}),(\mathrm{h},\mathrm{v}),(\mathrm{d},\mathrm{v})\}. \tag{2.4}$$

The set, S, is used so that equation (2.2) can be written concisely. The constants, c^l_{fg} ($l=1,2,3,4$ and $(f,g)\in S$), allow corners to be weighted. Like the z's, their values are at one's disposal. There are 24 of them. The terms in (2.2) correspond to those of figure 5. It is useful to define

$$\begin{aligned} c^1_{gf} &\equiv c^3_{gf}, & c^2_{fg} &\equiv -c^2_{gf}, \\ c^3_{fg} &\equiv c^1_{gf}, & c^4_{fg} &\equiv -c^4_{gf}, \end{aligned} \tag{2.5}$$

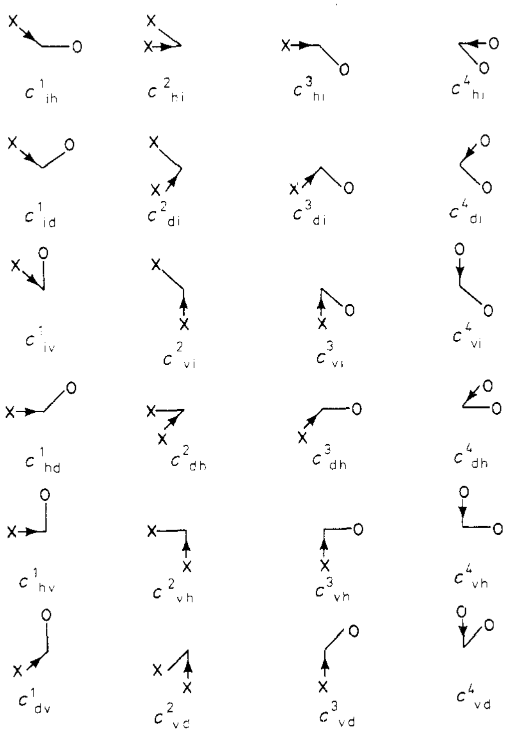

Figure 5. The 24 corner operators.

Table 1. The weights of the vertex configurations of the pseudo-free 128 vertex model. The Bloch wall Boltzmann factors have been extracted. The weights are expressed directly in terms of the parameters of the action (equations (2.1)–(2.3)) or via the functions in equations (2.8)–(2.21). Parts (*b*)–(*e*) of table 1 are given on the following pages.

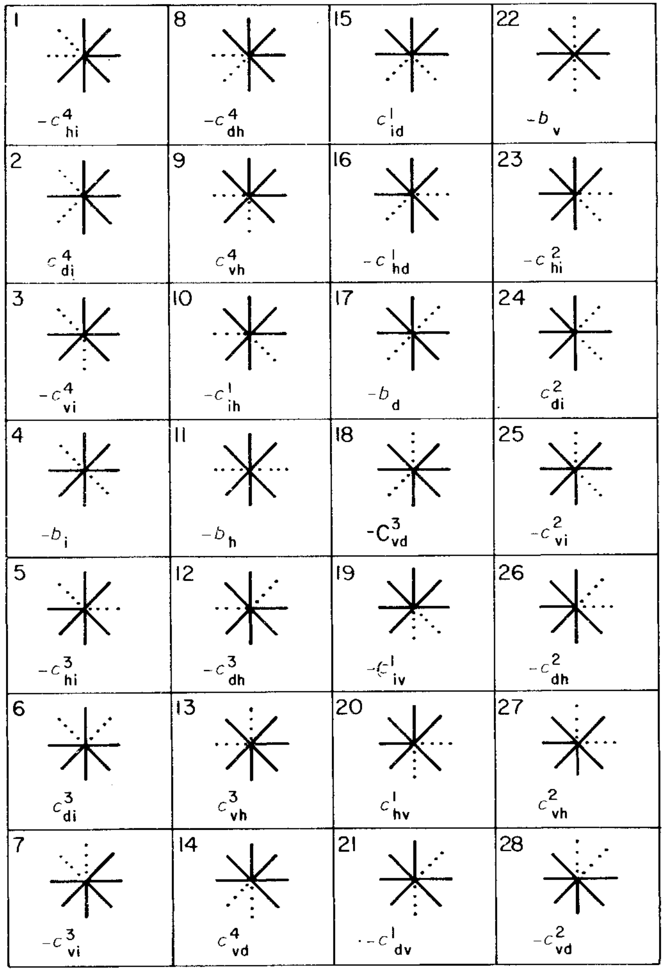

(*a*)

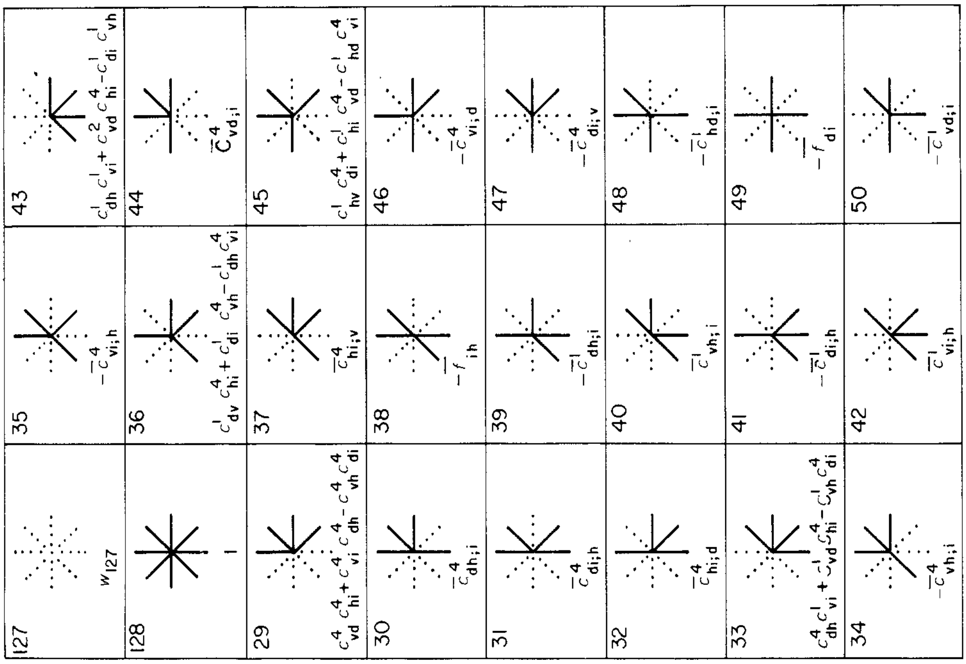

(b)

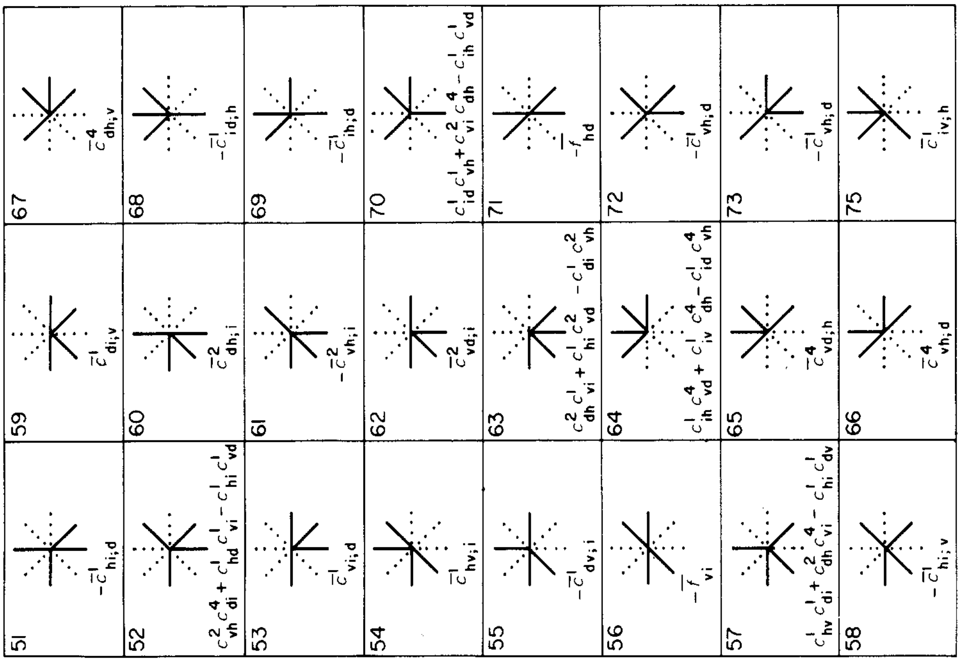

(c)

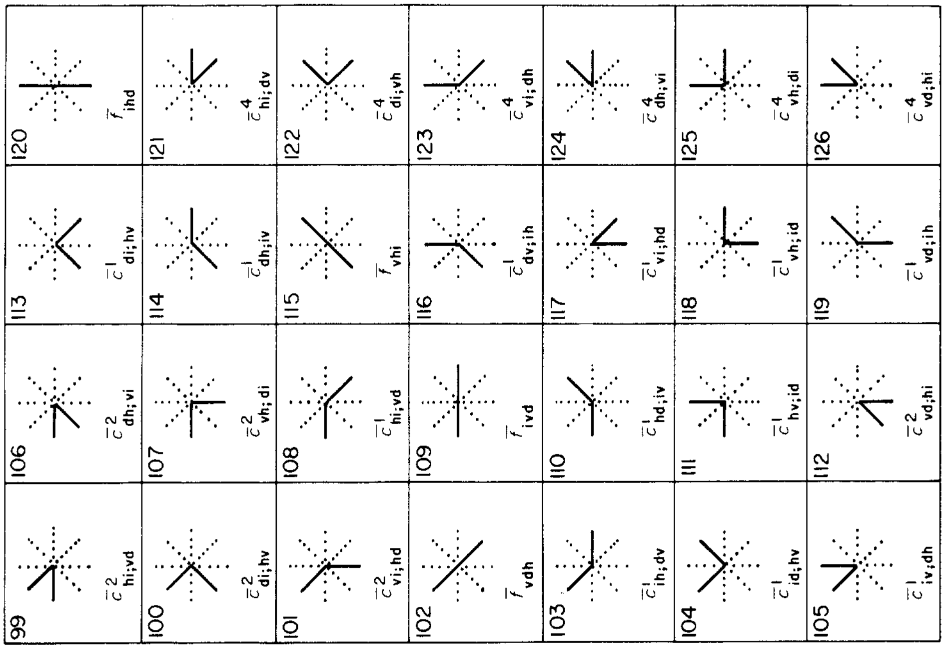

99 $\bar c^2_{hi;vd}$
100 $\bar c^2_{di;hv}$
101 $\bar c^2_{vi;hd}$
102 $\bar f_{vdh}$
103 $\bar c^1_{ih;dv}$
104 $\bar c^1_{id;hv}$
105 $\bar c^1_{iv;dh}$
106 $\bar c^2_{dh;vi}$
107 $\bar c^2_{vh;di}$
108 $\bar c^1_{hi;vd}$
109 $\bar f_{ivd}$
110 $\bar c^1_{hd;iv}$
111 $\bar c^1_{hv;id}$
112 $\bar c^2_{vd;hi}$
113 $\bar c^1_{di;hv}$
114 $\bar c^1_{dh;iv}$
115 $\bar f_{vhi}$
116 $\bar c^1_{dv;ih}$
117 $\bar c^1_{vi;hd}$
118 $\bar c^1_{vh;id}$
119 $\bar c^1_{vd;ih}$
120 $\bar f_{ihd}$
121 $\bar c^4_{hi;dv}$
122 $\bar c^4_{di;vh}$
123 $\bar c^4_{vi;dh}$
124 $\bar c^4_{dh;vi}$
125 $\bar c^4_{vh;di}$
126 $\bar c^4_{vd;hi}$

(*e*)

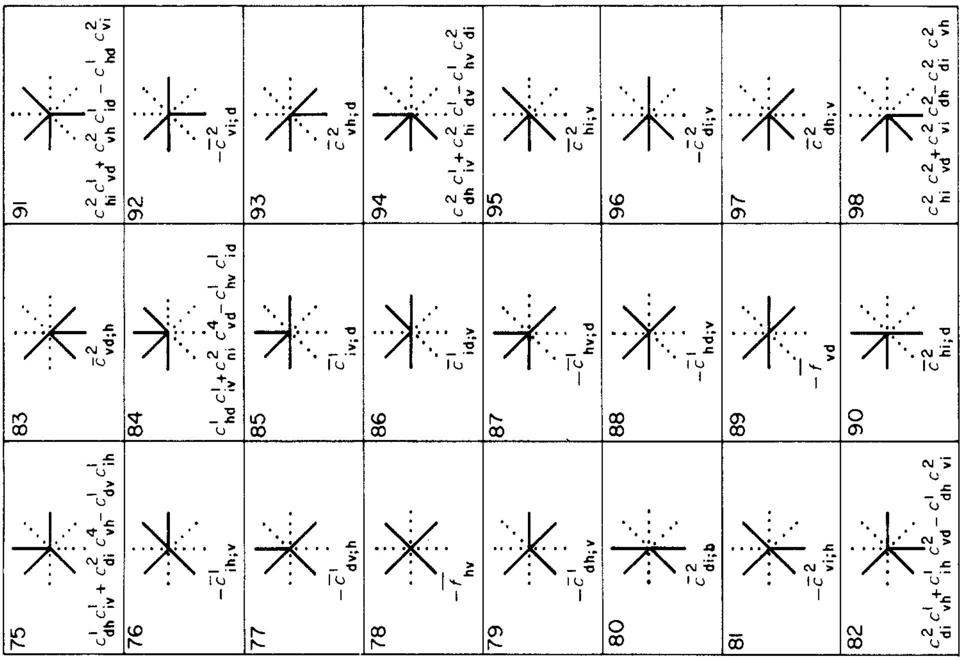

75 $c^1_{dh}c^1_{iv}+c^2_{di}c^4_{vh}-c^1_{dv}c^1_{ih}$
76 $-\bar c^1_{ih;v}$
77 $-\bar c^1_{dv;h}$
78 $-\bar f_{hv}$
79 $-\bar c^1_{dh;v}$
80 $\bar c^2_{di;b}$
81 $-\bar c^2_{vi;h}$
82 $c^2_{di}c^1_{vh}+c^1_{ih}c^2_{vd}-c^1_{dh}c^2_{vi}$
83 $\bar c^2_{vd;h}$
84 $c^1_{hd}c^1_{iv}+c^2_{hi}c^4_{vd}-c^1_{hv}c^1_{id}$
85 $\bar c^1_{iv;d}$
86 $\bar c^1_{id;v}$
87 $-\bar c^1_{hv;d}$
88 $-\bar c^1_{hd;v}$
89 $-\bar f_{vd}$
90 $\bar c^2_{hi;d}$
91 $c^2_{hi}c^1_{vd}+c^2_{vh}c^1_{id}-c^1_{hd}c^2_{vi}$
92 $-\bar c^2_{vi;d}$
93 $\bar c^2_{vh;d}$
94 $c^2_{dh}c^1_{iv}+c^2_{hi}c^1_{dv}-c^1_{hv}c^2_{di}$
95 $\bar c^2_{hi;v}$
96 $-\bar c^2_{di;v}$
97 $\bar c^2_{dh;v}$
98 $c^2_{hi}c^2_{vd}+c^2_{vi}c^2_{dh}-c^2_{di}c^2_{vh}$

(*d*)

for $(f, g) \in S$. Then,

$$A^{128}_{\text{corner}} = \sum_{\alpha\beta} \sum_{fg} \left(c^{1}_{fg} \eta^{f\dagger}_{\alpha\beta} \eta^{g}_{\alpha\beta} + \tfrac{1}{2} c^{2}_{gf} \eta^{g\dagger}_{\alpha\beta} \eta^{f\dagger}_{\alpha\beta} + \tfrac{1}{2} c^{4}_{gf} \eta^{g}_{\alpha\beta} \eta^{f}_{\alpha\beta} \right), \tag{2.6}$$

where the sum is over distinct f and g among the set {i, h, d, v}.

Equation (2.3) contains the monomer terms and the remaining four free parameters, b_{i}, b_{h}, b_{d}, and b_{v}.

In a functional integral these three actions draw polygons; A^{128}_{wall} draws the walls, A^{128}_{corner} forms corners, and A^{128}_{monomer} fills unfilled sites. The integral is an anticommuting variable one over the action, A_{128}:

$$A_{128} = A^{128}_{\text{wall}} + A^{128}_{\text{corner}} + A^{128}_{\text{monomer}}. \tag{2.7}$$

The pseudo-free 128 vertex model is a fermionic-like pseudo-free field theory.

By expanding the action, the CPPF configurations are obtained. Table 1 shows the weights of each vertex configuration after the Bloch wall Boltzmann factors have been extracted. It turns out that the overall sign of a vertex weight is determined by the number of line intersections as figure 6 illustrates. The total weight of any polygonal configuration is the product of table 1 vertex weights at each site times the Bloch wall Boltzmann factors, $z_f(f = \mathrm{i, h, d, v})$, for each unit of wall. Part (a) of table 1 has the configurations where six edges enter a site; (b)–(d) contain configurations with four lines entering; and (e) has those where two edges enter. The two remaining configurations, those with zero or eight lines entering (boxes 127 and 128), are placed at the top of part (b).

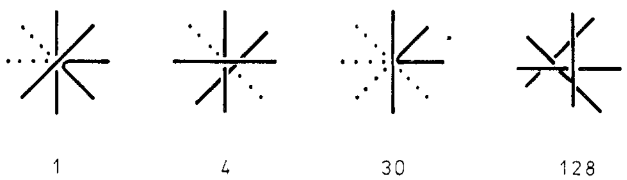

Figure 6. Overall minus signs. The configurations in boxes 1, 4, 30, and 128 of table 1 are reproduced here. They have been redrawn so that the intersections can be seen. If the number of intersections is even, the overall sign is positive, while an odd number of intersections yields a negative sign. Boxes 1, 4, 30, and 128 have respectively one, three, zero, and six intersections; hence boxes 1 and 4 have an overall minus sign, while boxes 30 and 128 do not.

One must be careful of minus signs which result from reordering the anticommuting variables. The Appendix proves that the overall sign of a closed non self-intersecting polygon is plus. The overall sign for intersecting polygons is $(-1)^I$, where I is the number of intersections. For intersections which occur at a vertex the minus sign factors have been included in the weights of table 1. There are, however, intersections which do not occur at a vertex (see figure 7). An additional minus sign factor must be included for each of these types of intersections.

The vertex weights are expressed in terms of the following coefficients:

$$c^{1}_{ef;g} \equiv c^{1}_{eg} c^{1}_{gf} - c^{2}_{ge} c^{4}_{fg}, \tag{2.8}$$

$$c^{2}_{ef;g} \equiv c^{1}_{eg} c^{2}_{gf} - c^{2}_{ge} c^{1}_{fg}, \tag{2.9}$$

$$c^{4}_{ef;g} \equiv c^{4}_{eg} c^{1}_{gf} - c^{1}_{ge} c^{4}_{fg}, \tag{2.10}$$

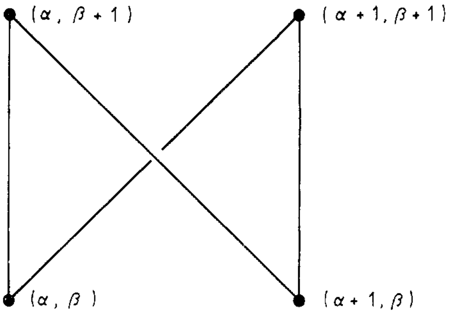

Figure 7. Extra minus sign. An extra minus sign factor results when any two sides intersect between lattice sites. This figure is an example in which this happens. The weight of this polygon is the product of Bloch wall Boltzmann factors, the product of table 1 vertex factors, times an extra minus one: $[z_i z_d z_h z_h]\times$[(box 105) (box 112) (box 117) (box 126)]$\times[-1]$.

$$\bar{c}^{\,l}_{ef;g} \equiv b_g c^{\,l}_{ef} + c^{\,l}_{ef;g}, \tag{2.11}$$

$$c^1_{ef;gj} \equiv c^1_{eg}c^1_{gf;j} - c^2_{ge}c^4_{fg;j} + c^1_{ej}c^1_{jf;g} - c^2_{je}c^4_{fj;g}, \tag{2.12}$$

$$c^2_{ef;gj} \equiv c^1_{eg}c^2_{gf;j} - c^2_{ge}c^1_{fg;j} + c^1_{ej}c^2_{jf;g} - c^2_{je}c^1_{fj;g}, \tag{2.13}$$

$$c^4_{ef;gj} \equiv c^4_{eg}c^1_{gf;j} - c^1_{ge}c^4_{fg;j} + c^4_{ej}c^1_{jf;g} - c^1_{je}c^4_{fj;g}, \tag{2.14}$$

$$\bar{c}^{\,l}_{ef;gj} \equiv c^{\,l}_{ef}\bar{F}_{gj} + b_j c^{\,l}_{ef;g} + b_g c^{\,l}_{ef;j} + c^{\,l}_{ef;gj}, \tag{2.15}$$

$$F_{fg} \equiv -c^1_{fg}c^1_{gf} + c^2_{fg}c^4_{gf}, \tag{2.16}$$

$$\bar{F}_{fg} \equiv b_f b_g + F_{fg}, \tag{2.17}$$

$$F_{efg} \equiv -c^1_{ef}c^1_{fe;g} + c^2_{ef}c^4_{fe;g} - c^1_{eg}c^1_{ge;f} + c^2_{eg}c^4_{ge;f}, \tag{2.18}$$

$$\bar{F}_{efg} \equiv b_e b_f b_g + b_e F_{fg} + b_f F_{eg} + b_g F_{ef} + F_{efg}, \tag{2.19}$$

$$\begin{aligned} F_{\mathrm{ihdv}} = (&-c^1_{\mathrm{id;h}}c^1_{\mathrm{di;v}} + c^2_{\mathrm{id;h}}c^4_{\mathrm{di;v}} - c^1_{\mathrm{iv;d}}c^1_{\mathrm{vi;h}} + c^2_{\mathrm{iv;d}}c^4_{\mathrm{vi;h}} \\ &- c^1_{\mathrm{ih;v}}c^1_{\mathrm{hi;d}} + c^2_{\mathrm{ih;v}}c^4_{\mathrm{hi;d}} - c^1_{\mathrm{iv;h}}c^1_{\mathrm{vi;d}} + c^2_{\mathrm{iv;h}}c^4_{\mathrm{vi;d}} \\ &- c^1_{\mathrm{ih;d}}c^1_{\mathrm{hi;v}} + c^2_{\mathrm{ih;d}}c^4_{\mathrm{hi;v}} - c^1_{\mathrm{id;v}}c^1_{\mathrm{di;h}} - c^2_{\mathrm{id;v}}c^4_{\mathrm{di;h}}). \end{aligned} \tag{2.20}$$

In equations (2.8)–(2.19), each e, f, g, and j stands for any of the i, h, d, and v. All subscripts must be distinct. In (2.11) and (2.15) $l = 1$, 2, or 4.

The coefficients satisfy the following symmetry properties: the c^2's, c^4's, $\bar{c}^2$'s, and $\bar{c}^4$'s are antisymmetric in the two indices before the semicolon and symmetric in the indices after the semicolon. For example, $c^2_{ef;g} = -c^2_{fe;g}$, $c^2_{ef;gj} = -c^2_{fe;gj} = c^2_{ef;jg} = -c^2_{fe;gj}$. The F's and $\bar{F}$'s are completely symmetric in their indices.

They have the following interpretation. Corners can combine to fill the anticommuting variable sites. F_{fg} (respectively, F_{efg} and F_{ihdv}) is the weight which results in filling the f and g (e, f, g and all) sites by using two (three and four) corners. F_{ihdv} excludes terms in which two pairs are filled separately, i.e. there is no term proportional to $F_{\mathrm{ih}}F_{\mathrm{dv}}$. $\bar{F}_{fg}$ (respectively, $\bar{F}_{efg}$) is the way f, g (e, f, g) sites can be filled by using monomers and corners.

Likewise, two corners can combine to form a third. $c^{\,l}_{ef;g}$ (respectively, $c^{\,l}_{ef;gj}$) is the way two (three) corners combine to form a $c^{\,l}_{ef}$ corner and in the process use up the g (g and j) variables. $\bar{c}^{\,l}_{ef;g}$ (respectively, $\bar{c}^{\,l}_{ef;gj}$) is the way a $c^{\,l}_{ef}$ corner can be formed, in which g (g and j) sites get filled, by using both monomers and corners.

All the definitions of functions in table 1 have been supplied except for the weight, w_{127}, of box 127. It is

$$w_{127} \equiv \bar{F}_{\mathrm{ihdv}} \equiv [(b_{\mathrm{i}} b_{\mathrm{h}} b_{\mathrm{v}} b_{\mathrm{d}}) + (b_{\mathrm{i}} b_{\mathrm{h}} F_{\mathrm{dv}} + b_{\mathrm{d}} b_{\mathrm{i}} F_{\mathrm{hv}} + b_{\mathrm{v}} b_{\mathrm{i}} F_{\mathrm{dh}} + b_{\mathrm{d}} b_{\mathrm{h}} F_{\mathrm{iv}} + b_{\mathrm{v}} b_{\mathrm{h}} F_{\mathrm{id}} + b_{\mathrm{v}} b_{\mathrm{d}} F_{\mathrm{ih}}) + (b_{\mathrm{i}} F_{\mathrm{hdv}} + b_{\mathrm{h}} F_{\mathrm{idv}} + b_{\mathrm{d}} F_{\mathrm{ivh}} + b_{\mathrm{v}} F_{\mathrm{idh}}) + (F_{\mathrm{ih}} F_{\mathrm{dv}} + F_{\mathrm{id}} F_{\mathrm{hv}} + F_{\mathrm{iv}} F_{\mathrm{dh}}) + (F_{\mathrm{ihdv}})]. \tag{2.21}$$

Table 1, along with figure 7, essentially defines the model.

3. The solution

The partition function can be related to a miniature dimer problem using the methods developed in II. If one, then, interchanges daggered and undaggered variables for $(-s, -t)$ variables, a determinant is obtained.

Define

$$\begin{aligned} \mathrm{i}(p_x, p_y) &= b_{\mathrm{i}} - z_{\mathrm{i}} \exp(\mathrm{i}p_x - \mathrm{i}p_y), & \mathrm{h}(p_x) &= b_{\mathrm{h}} - z_{\mathrm{h}} \exp(\mathrm{i}p_x), \\ \mathrm{d}(p_x, p_y) &= b_{\mathrm{d}} - z_{\mathrm{d}} \exp(\mathrm{i}p_x + \mathrm{i}p_y), & \mathrm{v}(p_y) &= b_{\mathrm{v}} - z_{\mathrm{v}} \exp(\mathrm{i}p_y). \end{aligned} \tag{3.1}$$

Let D be the following 8×8 diagonal matrix:

$$D(p_x, p_y) \begin{pmatrix} \mathrm{i}(p_x, p_y) & & & & & & & \\ & \mathrm{h}(p_x) & & & & & 0 & \\ & & \mathrm{d}(p_x, p_y) & & & & & \\ & & & \mathrm{v}(p_y) & & & & \\ & & & & \mathrm{i}(-p_x, -p_y) & & & \\ & 0 & & & & \mathrm{h}(-p_x) & & \\ & & & & & & \mathrm{d}(-p_x, -p_y) & \\ & & & & & & & \mathrm{v}(-p_y) \end{pmatrix}. \tag{3.2}$$

Let C^1, C^2, and C^4 be the following 4×4 arrays of numbers:

$$C^1 = \begin{pmatrix} 0 & c^1_{\mathrm{ih}} & c^1_{\mathrm{id}} & c^1_{\mathrm{iv}} \\ c^1_{\mathrm{hi}} & 0 & c^1_{\mathrm{hd}} & c^1_{\mathrm{hv}} \\ c^1_{\mathrm{di}} & c^1_{\mathrm{dh}} & 0 & c^1_{\mathrm{dv}} \\ c^1_{\mathrm{vi}} & c^1_{\mathrm{vh}} & c^1_{\mathrm{vh}} & 0 \end{pmatrix} \tag{3.3}$$

$$C^2 = \begin{pmatrix} 0 & c^2_{\mathrm{ih}} & c^2_{\mathrm{id}} & c^2_{\mathrm{iv}} \\ c^2_{\mathrm{hi}} & 0 & c^2_{\mathrm{hd}} & c^2_{\mathrm{hv}} \\ c^2_{\mathrm{di}} & c^2_{\mathrm{dh}} & 0 & c^2_{\mathrm{dv}} \\ c^2_{\mathrm{vi}} & c^2_{\mathrm{vh}} & c^2_{\mathrm{vd}} & 0 \end{pmatrix} \tag{3.4}$$

$$C^4 = \begin{pmatrix} 0 & c^4_{\mathrm{ih}} & c^4_{\mathrm{id}} & c^4_{\mathrm{iv}} \\ c^4_{\mathrm{hi}} & 0 & c^4_{\mathrm{hd}} & c^4_{\mathrm{hv}} \\ c^4_{\mathrm{di}} & c^4_{\mathrm{dh}} & 0 & c^4_{\mathrm{dv}} \\ c^4_{\mathrm{vi}} & c^4_{\mathrm{vh}} & c^4_{\mathrm{vd}} & 0 \end{pmatrix}. \tag{3.5}$$

Let $[C^1]^t$ denote the 4×4 matrix which is the transpose of C^1. Define the 8×8 matrix, $M(p_x, p_y)$, by

$$M(p_x, p_y) = D(p_x, p_y) + \begin{pmatrix} -[C^1]^t & [C^4] \\ [C^2] & [C^1] \end{pmatrix}, \tag{3.6}$$

and set

$$L(p_x, p_y) = \det M(p_x, p_y), \tag{3.7}$$

where det stands for the determinant. The partition function for the pseudo-free 128 vertex model, Z_{128}, in the thermodynamic limit, is

$$Z_{128} = \exp\left(T\tfrac{1}{2} \int_{-\pi}^{\pi} \frac{\mathrm{d}p_x}{2\pi} \int_{-\pi}^{\pi} \frac{\mathrm{d}p_y}{2\pi} \ln L(p_x, p_y) \right), \tag{3.8}$$

where T is the total number of sites. The free energy per site, f_{128}, is

$$-\beta f_{128} = \tfrac{1}{2} \int_{-\pi}^{\pi} \frac{\mathrm{d}p_x}{2\pi} \int_{-\pi}^{\pi} \frac{\mathrm{d}p_y}{2\pi} \ln L(p_x, p_y), \tag{3.9}$$

where β is the inverse temperature.

For particular models where the z's, c's, and b's take on certain values, the determinant in (3.7) can be evaluated by using computers. One can then obtain the free energy by using (3.9). Other physically interesting quantities such as the energy per site and the specific heat can be obtained by taking derivatives with respect to β.

4. The 128+8 pseudo-free vertex model

Closely related to the pseudo-free 128 vertex model is the 128+8 pseudo-free vertex model. Append to the lattice of figure 1 the points where inclined and diagonal bonds cross, that is, sites with half-integer cartesian coordinates. Figure 8(a) shows the original sites (the round ones) and the new half-integer sites (the square ones). The terms, round and square, or, integer and half-integer, will be used to distinguish the two types of sites. For round sites, bonds are drawn to the four nearest-neighbour round sites and the nearest-neighbour square sites, but, for square sites, bonds are drawn only

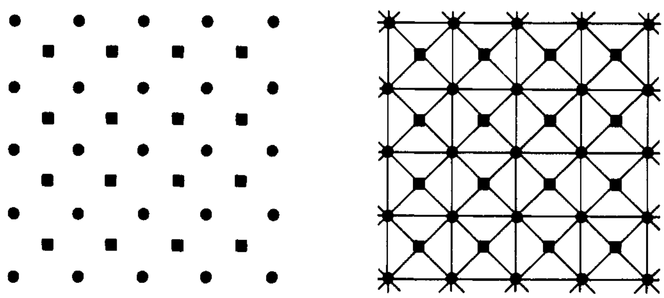

(a) (b)

Figure 8. (a) The 128+8 vertex model lattice. (b) The bonds in the 128+8 vertex model. The sites in figure 1(a) are the round ones here. In addition, sites have been added at the points with half-integer cartesian coordinates (the square sites).

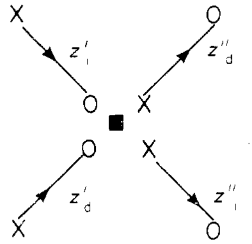

Figure 9. The diagonal and inclined wall operators. A square site has bonds connecting to the four nearest-neighbour round sites. This figure shows the four wall operators which produce these bonds. Each of the four has been assigned a separate weight.

to the four nearest-neighbour round sites (figure 8(*b*)). What is the most general easily solvable closed polygon partition function which can be drawn on the lattice of figure 8(*b*)? The answer is the 128+8 pseudo-free vertex model. This CPPF is required to have properties similar to the 128 vertex model: any number of polygons are allowed; they must be drawn on the lattice of figure 8(*b*), sides can intersect but cannot overlap; and the corners and sides are weighted by various factors. This CPPF is generated by using an anticommuting variable integral over an action, A_{128+8}. The action again consists of three pieces: one that draws the walls, $A^{128+8}_{\mathrm{wall}}$; one that forms corners, $A^{128+8}_{\mathrm{corner}}$; and one that fills unfilled anticommuting variable sites, $A^{128+8}_{\mathrm{monomer}}$.

$$A^{128+8}_{\mathrm{wall}}=\sum_{\alpha\beta}\left(z'_{\mathrm{d}}\eta^{\mathrm{d}\dagger}_{\alpha\beta}\eta^{\mathrm{d}}_{\alpha+\frac12\beta+\frac12}+z''_{\mathrm{d}}\eta^{\mathrm{d}\dagger}_{\alpha+\frac12\beta+\frac12}\eta^{\mathrm{d}}_{\alpha+1\beta+1}+z'_{\mathrm{i}}\eta^{\mathrm{i}\dagger}_{\alpha\beta+1}\eta^{\mathrm{i}}_{\alpha+\frac12\beta+\frac12}\right.$$
$$\left.+z''_{\mathrm{i}}\eta^{\mathrm{i}\dagger}_{\alpha+\frac12\beta+\frac12}\eta^{\mathrm{i}}_{\alpha+1\beta}+z_{\mathrm{h}}\eta^{\mathrm{h}\dagger}_{\alpha\beta}\eta^{\mathrm{h}}_{\alpha+1\beta}+z_{\mathrm{v}}\eta^{\mathrm{v}\dagger}_{\alpha\beta}\eta^{\mathrm{v}}_{\alpha\beta+1}\right). \tag{4.1}$$

The z_{h} and z_{v} wall operators are shown in figure 4, while the z'_{i}, z''_{i}, z'_{d}, z''_{d} wall operators are shown in figure 9. The weights of the two different kinds of diagonal bonds have been chosen independently; hence the two parameters z'_{d} and z''_{d}. The same goes for inclined bonds.

The corner action consists of a piece, $A^{128}_{\mathrm{corner}}$, identical to (2.2), and a piece that forms corners at square sites:

$$A^{128+8}_{\mathrm{corner}}=A^{128}_{\mathrm{corner}}+A^{8}_{\mathrm{corner}},$$

$$A^{8}_{\mathrm{corner}}=\sum_{\alpha\beta}\left(c^{1}\eta^{\mathrm{i}\dagger}_{\alpha+\frac12\beta+\frac12}\eta^{\mathrm{d}}_{\alpha+\frac12\beta+\frac12}+c^{2}\eta^{\mathrm{d}\dagger}_{\alpha+\frac12\beta+\frac12}\eta^{\mathrm{i}\dagger}_{\alpha+\frac12\beta+\frac12}+c^{3}\eta^{\mathrm{d}\dagger}_{\alpha+\frac12\beta+\frac12}\eta^{\mathrm{i}}_{\alpha+\frac12\beta+\frac12}\right.$$
$$\left.+c^{4}\eta^{\mathrm{d}}_{\alpha+\frac12\beta+\frac12}\eta^{\mathrm{i}}_{\alpha+\frac12\beta+\frac12}\right). \tag{4.2}$$

The round corner operators are shown in figure 5, while the square corner ones are shown in figure 10.

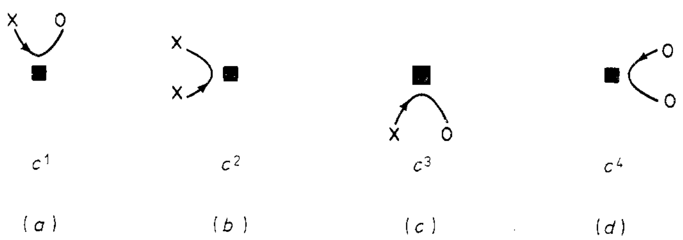

Figure 10. The four corner operators at a square site.

Finally, the monomer action consists of a piece, A^{128}_{monomer}, which fills round anticommuting variable sites, and a piece which fills square sites:

$$A^{128+8}_{\text{monomer}} = A^{128}_{\text{monomer}} + A^{8}_{\text{monomer}},$$

$$A^{8}_{\text{monomer}} = \sum_{\alpha\beta} (m_{\text{i}} \eta^{\text{i}}_{\alpha+\frac{1}{2}\,\beta+\frac{1}{2}} \eta^{\text{i}\dagger}_{\alpha+\frac{1}{2}\,\beta+\frac{1}{2}} + m_{\text{d}} \eta^{\text{d}}_{\alpha+\frac{1}{2}\,\beta+\frac{1}{2}} + \eta^{\text{d}\dagger}_{\alpha+\frac{1}{2}\,\beta+\frac{1}{2}}), \tag{4.3}$$

where A^{128}_{monomer} is given in (2.3).

At round sites there are four kinds of anticommuting variables: inclined, horizontal, diagonal, and vertical, whereas at square sites there are only two kinds: inclined and diagonal.

The result is a vertex model with two kinds of vertices: square and round. The weights of the round vertices are the same as for the pseudo-free 128 vertex model and are given in table 1. The weights of the square vertices are the same as the pseudo-free eight vertex model (i.e. free-fermion model) and are given in table 2. All wall weights have been extracted, so that the total weight is the vertex weights times the wall weights. If $m_{\text{i}} = m_{\text{d}} = 1$ and $c^1 = c^2 = c^3 = c^4 = 0$, the pseudo-free 128 vertex model is obtained along with the minus sign factor of figure 7.

Table 2. The weights of the square vertices in the 128 + 8 pseudo-free vertex model.

(a)		$(m_{\text{i}} m_{\text{d}} - c^1 c^3 - c^2 c^4)$	(e)		c^2
(b)		m_{i}	(f)		c^3
(c)		m_{d}	(g)		c^4
(d)		c^1	(h)		-1

In the Appendix, it is proven that non self-intersecting polygons have no overall minus signs due to reorderings of anticommuting variables. For intersecting polygons, a (-1) results for each intersection. These minus sign factors have been absorbed into the weights of tables 1 and 2.

The 128 + 8 pseudo-free model has 40 parameters. The anticommuting variable integrals over square sites can be performed since they do not couple to each other. The result is

$$\prod_{\alpha\beta} (f + m_{\text{i}} z'_{\text{d}} z''_{\text{d}} \eta^{\text{d}\dagger}_{\alpha\beta} \eta^{\text{d}}_{\alpha+1\,\beta+1} + m_{\text{d}} z'_{\text{i}} z''_{\text{i}} \eta^{\text{i}\dagger}_{\alpha\beta+1} \eta^{\text{i}}_{\alpha+1\,\beta} + z'_{\text{i}} c^1 z''_{\text{d}} \eta^{\text{i}\dagger}_{\alpha\beta+1} \eta^{\text{d}}_{\alpha+1\,\beta+1}$$
$$+ z'_{\text{d}} c^2 z'_{\text{i}} \eta^{\text{d}\dagger}_{\alpha\beta} \eta^{\text{i}\dagger}_{\alpha\beta+1} + z'_{\text{d}} c^3 z''_{\text{i}} \eta^{\text{d}\dagger}_{\alpha\beta} \eta^{\text{i}}_{\alpha+1\,\beta} + z''_{\text{d}} c^4 z''_{\text{i}} \eta^{\text{d}}_{\alpha+1\,\beta+1} \eta^{\text{i}}_{\alpha+1\,\beta}$$
$$+ z'_{\text{i}} z''_{\text{i}} z'_{\text{d}} z''_{\text{d}} \eta^{\text{d}\dagger}_{\alpha\beta} \eta^{\text{d}}_{\alpha+1\,\beta+1} \eta^{\text{i}\dagger}_{\alpha\beta+1} \eta^{\text{i}}_{\alpha+1\,\beta}), \tag{4.4}$$

which can be written as

$$f^T \exp\left[\sum_{\alpha\beta} (z_{\rm d}\eta^{\rm d\dagger}_{\alpha\beta}\eta^{\rm d}_{\alpha+1\,\beta+1} + z_{\rm i}\eta^{\rm i\dagger}_{\alpha\beta+1}\eta^{\rm i}_{\alpha+1\,\beta} + k^1_{\rm id}\eta^{\rm i\dagger}_{\alpha\beta}\eta^{\rm d}_{\alpha+1\,\beta}\right.$$
$$\left. + k^2_{\rm di}\eta^{\rm d\dagger}_{\alpha\beta}\eta^{\rm i\dagger}_{\alpha\beta+1} + k^3_{\rm di}\eta^{\rm d\dagger}_{\alpha\beta}\eta^{\rm i}_{\alpha+1\,\beta} + k^4_{\rm di}\eta^{\rm d}_{\alpha\beta}\eta^{\rm i}_{\alpha\beta-1})\right], \tag{4.5}$$

where T is the total number of (square) sites and

$$f \equiv m_{\rm i}m_{\rm d} - c^1c^3 - c^2c^4, \qquad z_{\rm d} \equiv z'_{\rm d}z''_{\rm d}m_{\rm i}/f, \qquad z_{\rm i} \equiv z'_{\rm i}z''_{\rm i}m_{\rm d}/f,$$
$$k^1_{\rm id} \equiv z'_{\rm i}z''_{\rm d}c^1/f, \qquad k^2_{\rm di} \equiv z'_{\rm d}z'_{\rm i}c^2/f \tag{4.6}$$
$$k^3_{\rm di} \equiv z'_{\rm d}z''_{\rm i}c^3/f, \qquad k^4_{\rm di} \equiv z''_{\rm d}z''_{\rm i}c^4/f.$$

It is useful to define

$$k^1_{\rm di} \equiv k^3_{\rm di}, \qquad k^2_{\rm id} \equiv -k^2_{\rm di}, \tag{4.7}$$
$$k^4_{\rm id} \equiv -k^4_{\rm di}, \qquad \ln f = -\beta f^0_{128+8}.$$

The k^l_{fg}($l = 1$, 2, 3, or 4; f, g = i or d) terms in (4.5) have the pictorial representation given in figure 11. The resulting anticommuting variable action is the same as for the pseudo-free 128 vertex model except for the four k^l_{fg} terms, and the fact that $z_{\rm d}$ and $z_{\rm i}$ are related to square site parameters via equation (4.6).

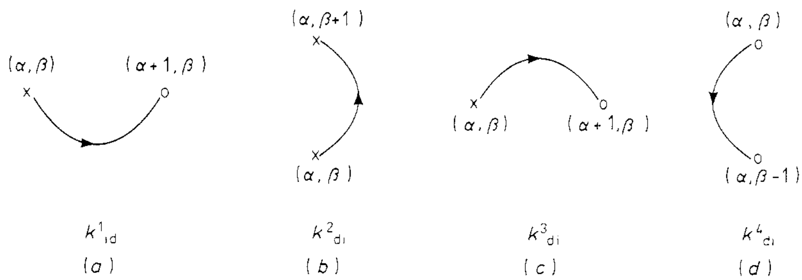

Figure 11. The k^l_{fg} operators. After square site integrals have been performed, the 128 + 8 vertex model becomes the 128 vertex model with the addition of these four terms.

Let $D(p_x, p_y)$, C^1, C^2 and C^4 be the same matrices as in equations (3.2), (3.3), (3.4) and (3.5). Define

$$K^1(p_x) = \begin{pmatrix} 0 & 0 & k^1_{\rm id}\exp(-{\rm i}p_x) & 0 \\ 0 & 0 & 0 & 0 \\ k^1_{\rm di}\exp(-{\rm i}p_x) & 0 & 0 & 0 \\ 0 & 0 & 0 & 0 \end{pmatrix} \tag{4.8}$$

$$K^2(p_y) = \begin{pmatrix} 0 & 0 & k^2_{\rm id}\exp({\rm i}p_y) & 0 \\ 0 & 0 & 0 & 0 \\ k^2_{\rm di}\exp(-{\rm i}p_y) & 0 & 0 & 0 \\ 0 & 0 & 0 & 0 \end{pmatrix} \tag{4.9}$$

$$K^4(p_y) = \begin{pmatrix} 0 & 0 & k^4_{\mathrm{id}} \exp(-\mathrm{i}p_y) & 0 \\ 0 & 0 & 0 & 0 \\ k^4_{\mathrm{di}} \exp(\mathrm{i}p_y) & 0 & 0 & 0 \\ 0 & 0 & 0 & 0 \end{pmatrix}. \tag{4.10}$$

Let $[K^1(p_x)]^\dagger$ denote the Hermitian conjugate of $K^1(p_x)$, i.e. $[K^1(p_x)]^\dagger = [K^1(-p_x)]^{\mathrm{t}}$. Let

$$M_{128+8}(p_x, p_y) = D(p_x, p_y) + \begin{pmatrix} -[C^{1\mathrm{t}} + K^1(p_x)^\dagger] & [C^4 + K^4(p_y)] \\ [C^2 + K^2(p_y)] & [C^1 + K^1(p_x)] \end{pmatrix} \tag{4.11}$$

$$L_{128+8}(p_x, p_y) = \det M_{128+8}(p_x, p_y). \tag{4.12}$$

Then, the free energy per unit site, f_{128+8}, (that is, per round and square site pair) is

$$-\beta f_{128+8} = -\beta f^0_{128+8} + \tfrac{1}{2} \int_{-\pi}^{\pi} \mathrm{d}p_x/2\pi \int_{\pi}^{\pi} \mathrm{d}p_y/2\pi \ln L_{128+8}(p_x, p_y), \tag{4.13}$$

where f^0_{128+8} is given in (4.7)

5. Conclusion

Two new statistical mechanics models have been solved. They are solvable via the Pfaffian method, although this paper solves them using the anticommuting variables.

The next step is to determine the physics of these models, in particular, the critical phenomenon. Because of the 8×8 determinants in equations (3.7) and (4.12), this will be quite tedious. The use of computers to evaluate these determinants will probably be necessary. One can say, however, that there will be multiple phase transitions with Ising-like logarithmically divergent specific heat. This is because one submodel, the pseudo-free 32 vertex model, is known to have such multiple phase transitions (Sacco and Wu 1975)

Acknowledgments

I thank Harry Morrison for reading the manuscript and making useful suggestions. I also thank Luanne Neumann for the typing.

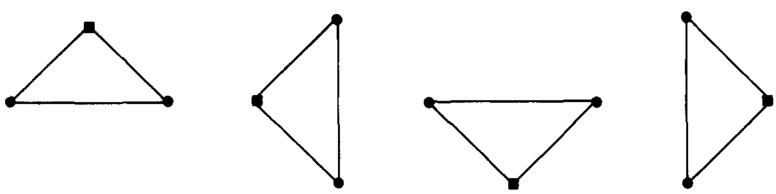

(a) (b) (c) (d)

Figure 12. The four elementary triangles of the lattice of figure 8(*b*).

Appendix. Overall minus signs: the non self-intersecting polygons

This Appendix will prove that there are no overall minuses created by reorderings of anticommuting variables for a non self-intersecting polygon drawn on the 128+8

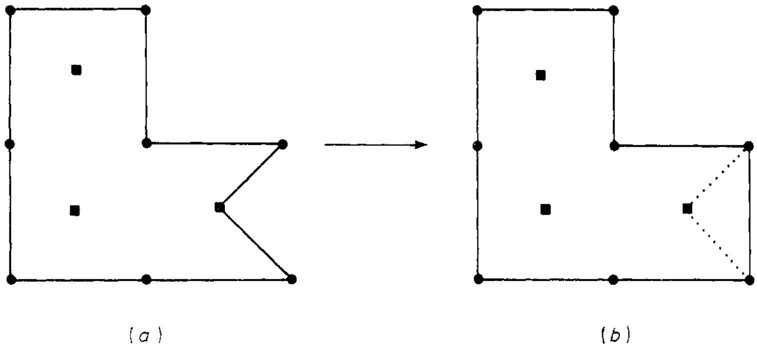

Figure 13. Building up a polygon from elementary triangles. The polygon of figure (*b*) is obtained from the polygon of figure (*a*) by attaching the elementary triangle of figure 12(*b*).

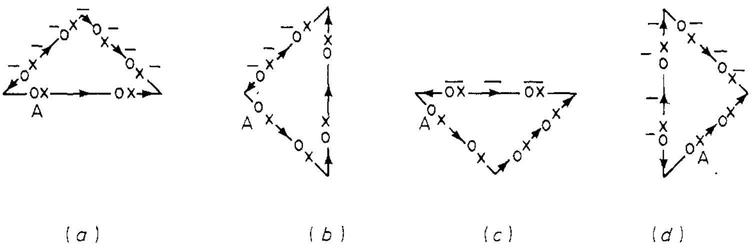

Figure 14. The overall sign of the elementary triangles. The sign is determined by the sign rules of figure 8 of paper I. Begin at the x near the point A, and proceed counterclockwise around the triangle. The minuses due to rules (a) and (b) are shown here. In each figure there are an odd number of them. In addition there is a minus due to rule (*c*). Thus the overall sign of each of the four elementary triangles is plus.

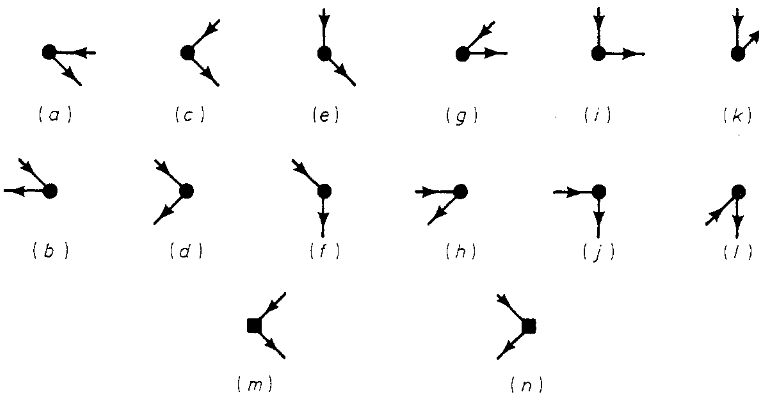

Figure 15. The oriented corners which create a minus sign. Figures (*a*) through (*l*) (respectively, figures (*m*) and (*n*)) show the round (square) vertex corners which create a minus sign because of anticommuting variable reordering.

lattice of figure 8(*b*). This also proves the result for the pseudo-free 32 vertex and pseudo-free 128 vertex models since any polygon drawn on their lattice can be drawn on the 128 + 8 lattice and the same kinds of bilinear operators are used.

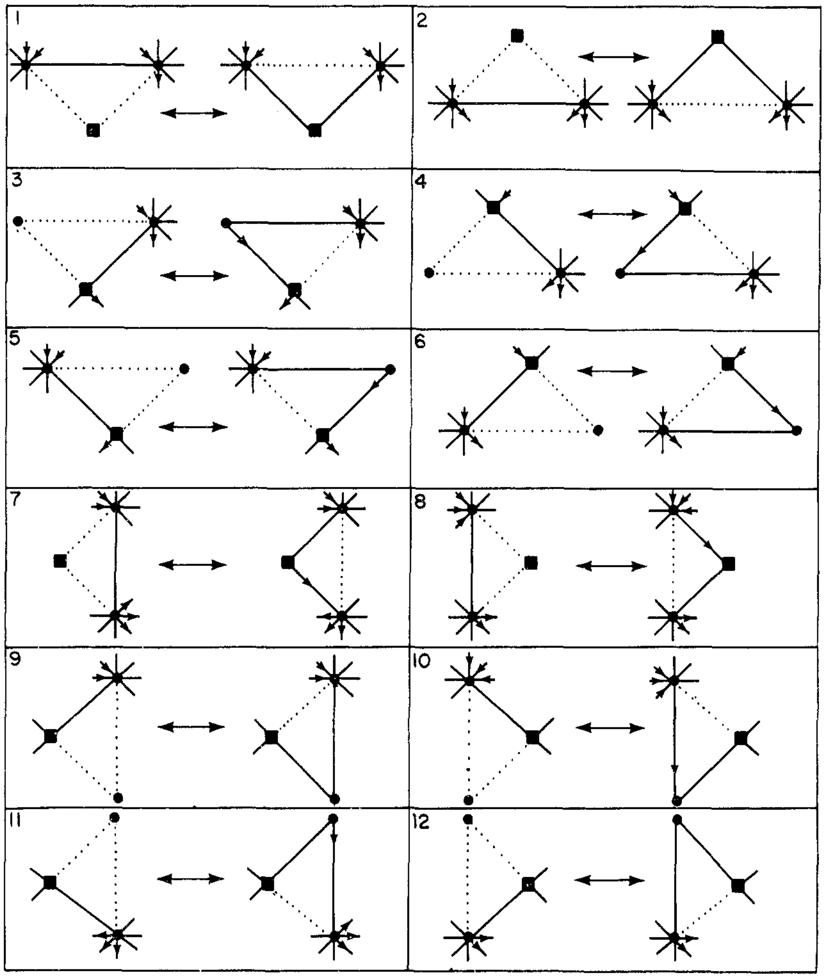

Figure 16. The 480 cases. Here are the 480 cases which must be considered in the induction step. Each of the 12 boxes shows two of the 24 ways of appending an elementary triangle. In the left half of a box one side is joined, while in the right half two sides are joined. The joining triangle is the one formed by the solid and dotted edges. Only the neighbouring structure of the polygon, to which the elementary triangle is being attached, is shown. When this triangle is attached to a configuration on the left, a configuration on the right results (see figure 17(*a*), which is an example for box 1), and when this triangle is attached to a configuration on the right a configuration on the left results (see figure 17(*b*), which is an example for box 1, and figure 13 which is an example for box 7). An arrow on a line indicates that when the orientation is in that direction, then one of the figure 15 corners is involved and a minus factor is present. Box 1 shows that the corner minus sign structure is unchanged in the joining process. Sometimes the process creates (or removes) a figure 15 corner; however another one is always created or removed at one of the two other vertices (see figure 17(*c*), which is a subcase of box 6). By inspecting these boxes, corner minus sign factors are seen to be created or removed in pairs so that the overall minus sign factor is unchanged.

The proof is similar to that for the free-fermion model, which was given in Appendix B of I to which the reader is referred. Extensive use will be made of the sign rules (a), (b), and (c) of figure 8 of paper I. The proof proceeds via induction on the area of a polygon. Any polygon can be built from the four elementary triangles of figure 12 (see figure 13). These are the polygons of minimum area. Figure 14 starts the induction process by proving that these have an overall plus sign.

As required by the sign rules, the polygon is given an orientation. Choose the starting point to be on x. Move around the polygon and count the number of minus signs due to rules (a) and (b). When moving in the positive directions of figure 2, no minus signs occur because the x's are after the o's and arrows point in the correct directions. When moving in the negative directions, there is a minus sign factor because the x's occur before the o's, but, in addition, there is a minus sign factor because arrows point in the wrong direction. Moving in straight lines causes no minuses. Next consider corners. There are 56 different corners; the 28 types of figures 5 and 10 are multiplied by two orientations. Figure 15 summarises the results. The corners of figure 15 create a minus sign and all others do not. The easy way to find the overall minus sign is to count the number of figure 15 corners in an oriented polygon. If the number is odd, then the extra minus due to rule (c) makes the overall sign positive.

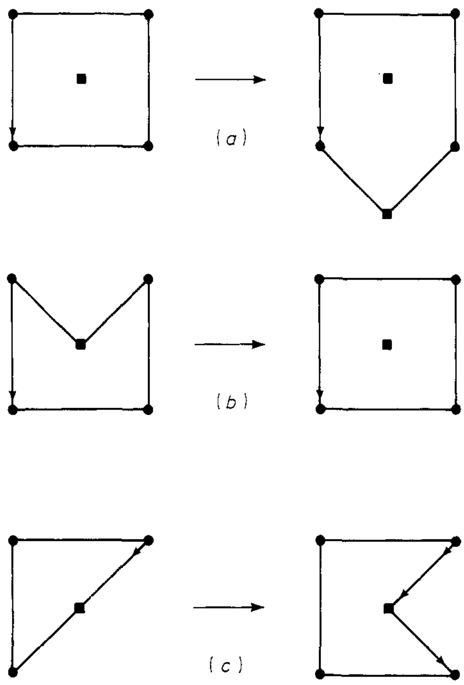

Figure 17. Examples of the figure 16 induction step. Figure (*a*) is an example of going from a box 1 left configuration to a box 1 right configuration. Figure (*b*) shows a box 1 right configuration going to a box 1 left configuration. The arrows denote the location of a figure 15 corner when traversing the polygons in a counterclockwise direction. In figures (*a*) and (*b*) no new figure 15 corners are created. Figure (*c*) is an example of a box 6 transformation where two extra figure 15 corners are created, when the polygon is oriented in the clockwise direction.

The elementary triangles can be attached to polygons in 24 different ways: each of the four elementary triangles can attach one side or two sides in three ways. All twenty-four are illustrated in figure 16. Each of these results in several cases depending on the neighbouring structure where the triangle is joined. In total, there are 480 different cases to consider. These are all shown in figure 16. It is found that the addition of an elementary polygon creates zero or two minus factors or removes two minus factors. This implies that the overall minus sign factor due to corners is the same as for the elementary triangles, namely minus. The number of corner minuses is odd. When combined with the rule (c) minus, the claim is proved: a non self-intersecting polygon has no minus signs due to reorderings of anticommuting variables.

References

Samuel S 1978a *The Use of Anticommuting Integrals in Statistical Mechanics I, LBL preprint* 8217 (1980 *J. Math. Phys.* to be published November)

—— 1978b *The Use of Anticommuting Integrals in Statistical Mechanics II, LBL preprint* 8300 (1980 *J. Math. Phys.* to be published November)

Sacco J E and Wu F Y 1975 *J. Phys. A: Math Gen.* **8** 1780

Schultz T D, Mattis D C and Lieb E H 1964 *Rev. Mod. Phys.* **36** 856